Development of a Three-Dimensional Viscous-Inviscid coupling Method for Wind Turbine Computations

Ramos García, Néstor; Sørensen, Jens Nørkær; Shen, Wen Zhong

Published in:
Proceedings of the 2013 International Conference on aerodynamics of Offshore Wind Energy Systems and wakes (ICOWES2013)

Publication date:
2013

DEVELOPMENT OF A THREE-DIMENSIONAL VISCOUS-INVISCID COUPLING METHOD FOR WIND TURBINE COMPUTATIONS

Néstor Ramos García , Jens Nørkær Sørensen and Wen Zhong Shen
Department of Wind Energy, Fluid Mechanics Section, Building 403,
Technical University of Denmark, DK-2800 Lyngby Denmark,
E-mail: nerga@dtu.dk

June 7, 2013

Abstract

$MIRAS$, a computational model for predicting the aerodynamic behavior of wind turbine blades and wakes subject to unsteady motions and viscous effects has been developed. The model is based on a three-dimensional panel method using a surface distribution of quadrilateral singularities with a Neumann no penetration condition. Viscous effects inside the boundary layer are taken into account through the coupling with the quasi-3D integral boundary layer solver Q^3UIC. A free-wake model is employed to simulate the vorticity released by the blades in the wake. In this paper simulations are presented in an effort to validate the code for three different rotor geometries, the MEXICO experiment rotor, the DELFT rotor and the NREL 5MW rotor.

1 Introduction

GPU and parallel computing, endless terabytes of memory, high speed connections, and other aspects of computer resources have become more powerful and accessible in recent years. However it is still behind our limits to use Navier-Stokes simulations for the design of wind turbines due to the large amount of computations involved in an optimization procedure. The free-wake vortex methods, extensively studied during the last four decades [1] [7] [2] [3], are now a mature tool with the potential to become the new generation of fast-tools for analysis and design of wind turbines. This type of code permits a direct interaction between the design procedure and the blade geometry (CAD) with a low computational cost. Unlike Navier-Stokes codes that need to solve the entire flow domain, panel methods can simulate the flow around a complex geometry by distributing singularity elements on the body surface. Panel methods become even more attractive by the possibility of solving the integral boundary layer equations and take into account the viscous effects using the transpiration velocity concept [4].

Wind turbine wake is a key element in the performance of rotor blade aerodynamics, having a strong influence in the rotor plane. From an engineering point of view, the free-wake vortex

approach is suitable to accurately model the inviscid phenomena that drives the general characteristics of the flow in the rotor wake, including the blade root and tip vortices, which are the most dominant structures in the wake. The basic free-wake vortex filament method consist of infinitely thin vortex filaments. To avoid numerical singularities, previous researchers have applied a viscous core model, modeling in this way a more physical distribution of the velocities induced by each one of the vortex filaments that forms the wake, desingularizing in this way the Biot-Savart law near the center of the filament, [8]. The diffusive time scales can be represented by changes in the vortex core radius as a function of the vortex age, using a turbulence eddy viscosity parameter [15]. Other improvements in the viscous core model include the introduction of changes in vortex strength due to filament stretching or squeezing, Ananthan and Leishman [9].

It is known that the viscous effects are important in the area surrounding the body surface, the boundary layer, playing a key role in the blade aerodynamics, especially at high angles of attack just before and after separation takes place. During the last decades simplified approaches to resolve the boundary layer equations have been developed by many researchers. In the two-dimensional case, panel methods have evolved to include viscous effects by solving the boundary layer in an integral manner, [10], [11] and [12] amongst others. Recently the Quasi-3D Unsteady Interactive Code Q^3UIC was developed by Ramos-García et al. [5] [6] to take into account the rotational effects arising from Coriolis and centrifugal forces. In the three-dimensional case, various researchers have previously implemented a viscous-inviscid coupling using the strip theory approach. Cebeci et al[20] combined a three-dimensional panel method with an inverse finite-difference boundary layer solver. Pesonen et al [21] and Lemmerman et al [22] coupled a three-dimensional panel method with an integral boundary layer solver. To the knowledge of the authors the present method has not yet been applied for the study of wind turbine aerodynamics and its wake dynamics.

In the present work a zonal viscous-inviscid coupling method is developed in which the inviscid part is composed by a three-dimensional panel method with a free-wake model, the viscous effects confined inside the boundary layer are computed with the integral boundary layer solver Q^3UIC. This viscous-inviscid interactive code will be referred as $MIRAS$, Method for viscous-inviscid Interactive Rotor Aerodynamic Simulations. In what follows $MIRAS$ is used to simulate the DELFT and MEXICO wind turbine model rotors and the NREL 5MW virtual rotor, simulated aerodynamic forces and wake velocities have been compared against experiments and Navier-Stokes simulations.

2 Governing equations

A wind turbine rotor is usually composed by two or three blades, their rotation generates a spiral vortex wake convected downstream. The rotor wake is formed by strong vortex structures and has a large impact in the aerodynamics of the rotor itself. To simulate the flow around a wind turbine rotor, we use a viscous-inviscid coupling method where the inviscid flow around the wind turbine rotor is solved using a panel method to simulate the blades, in which the viscous effects are taken into account by the Q^3UIC code. The wake is modeled by vortex filaments

released at the blades trailing edges in form of straight lines and convected downstream using the Biot-Savart law.

In the following paragraphs the theory behind this approach will be introduced briefly. For more detailed information about the model, the the reader is referred to Ramos-Garcia et al [5] [6].

For a potential flow around a solid body with surface S, the velocity at a point P in the flow domain can be expressed as a superposition of the undisturbed translating velocity, $\underline{U_\infty}$, and the disturbance velocity created by the solid body, $\underline{U_p}$, resulting in

$$\underline{U_I} = \underline{U_\infty} + \underline{U_p} \tag{1}$$

If the flow is considered to be incompressible, inviscid and irrotational, $\underline{U_p}$ can be expressed as

$$\underline{U_p} = -\nabla\phi \tag{2}$$

where ϕ is a potential function that satisfies the Laplace equation

$$\nabla^2\phi = 0 \tag{3}$$

As the solid body surface S is impermeable, the normal component of the velocity must be zero at the wall which gives a Neumann condition of no penetration across the body

$$\frac{\partial\phi}{\partial n} = \nabla\phi \cdot \underline{n} = \underline{U_\infty} \cdot \underline{n} \tag{4}$$

In practice, the problem is considered in two regions, the solid body and the downstream wake. The body is simulated by a distribution of quadrilateral surface dipoles, μ, and quadrilateral sources, σ. An extra source distribution, σ_{wT}, equal to the transpiration velocity computed with Q^3UIC, is introduced to account for viscous effects confined inside the boundary layer. The first row of wake elements is simulated using quadrilateral panel dipoles while further downstream the panels are converted into wake elements formed by straight line vortex filaments, Γ.

$$\nabla\Phi = \frac{-1}{4\pi}\int_b (\sigma + \sigma_{wT})\,\nabla\left(\frac{1}{r}\right) + \frac{1}{4\pi}\int_b \mu\nabla\left[\frac{\partial}{\partial n}\left(\frac{1}{r}\right)\right] + \frac{1}{4\pi}\int_w \Gamma\,\nabla\left[\frac{\partial}{\partial n}\left(\frac{1}{r}\right)\right] + \nabla\Phi_\infty \tag{5}$$

The vortex wake is released at the bodies trailing edges using the unsteady Kutta-Joukowsky condition of zero trailing edge loading. To satisfy this condition, at each time step a quadrilateral panel with a doublet distribution is created as the first wake panel for each one of the span-wise stations. The strength of these panels, $\underline{\Gamma_{fst}}$, is equal to the difference between the corresponding upper and lower trailing edge quadrilateral doublets

$$\underline{\Gamma_{fst}} = \underline{\mu_u} - \underline{\mu_l} \tag{6}$$

Following Katz and Plotkin [7] the first wake panel is convected downstream from the trailing edge with a 30% of the local undisturbed velocity. Downstream of the first row of wake panels the quadrilateral doublets are transformed into vortex filaments and clustered into vortex

elements. The strength of the vortex filaments remains constant in time with their motion represented by Lagrangian fluid markers placed at its end points which are convencted downstream with the total velocity $\underline{\mathbf{u}}$

$$\underline{\mathbf{u}} = \underline{\mathbf{u}}_{\infty} + \underline{\mathbf{u}}_{body} + \underline{\mathbf{u}}_{wake} \tag{7}$$

where $\underline{\mathbf{u}}_{\infty}$ is the freestream velocity, $\underline{\mathbf{u}}_{body}$ is the influence of the solid body and $\underline{\mathbf{u}}_{wake}$ is the induction created by the other wake elements.

The velocity induced by the wake vortex filaments is computed by applying the Biot-Savart law. In order to desingularize its behavior as $\mathbf{r}$ tends to zero the Biot-Savart formula is modified following Leishman et al. [13]. Where a viscous core is applied to all the released vortex filaments during the time updating procedure. Therefore, an approximation to viscous diffusion, vortex core growth and vortex straining is included modifying the Biot-Savart law as follows

$$\mathbf{u}_{wake} = K\frac{\Gamma}{4\pi}\frac{\underline{\mathbf{dl}} \times \underline{\mathbf{r}}}{|\underline{\mathbf{r}}|^3} \tag{8}$$

where K is the kernel parameter, which uses the Scully profile account for the vortex filament viscous core [14]. To include the core growth rate, Squire model is applied by introducing the turbulent eddy viscosity parameter [15]. Following Bhagwat and Leishman a straining model has been implemented to take into account the change in vortex filament radius due to its variations in length, stretching or squeezing [16].

Once the wake updating procedure is finalized, the new solution for the solid body singularities is calculated. Knowing the doublets, μ, the local inviscid perturbation velocities are calculated using a nodal interpolation of the doublets strength. Finally, the unsteady Bernoulli equation is used to compute the surface pressure on each one of the rotor blades,

$$\frac{\partial \underline{\phi}}{\partial t} + \frac{1}{2}|\underline{\mathbf{v}}|^2 + \frac{1}{\rho}\underline{p} = +\frac{1}{\rho}\underline{p}_{ref} \tag{9}$$

Viscous-inviscid coupling

The viscous boundary layer is solved by using the in-house Q^3UIC code. Q^3UIC is an aerodynamic tool developed to solve the quasi three-dimensional integral boundary layer equations, [5] [6]. The model is based on a viscous-inviscid interaction technique using strong coupling between the viscous and inviscid parts. In Q^3UIC, the inviscid part is solved using a two-dimensional potential flow panel method and the viscous effects are taken into account by solving the integral form of the boundary layer $r-$ and $\theta-$ momentum equations with extension for three-dimensional rotational effects created by Coriolis and centrifugal forces.

The r and θ integral momentum boundary layer equations can be written in terms of the boundary layer edge velocity, u_e, and the integral boundary layer parameters $\theta_1, \theta_2, \delta_1^*, \delta_2^*, \delta, \delta_3, H, C_f$ and β_w as:

$$\frac{\partial \theta_1}{\partial s} = -\frac{1}{u_e^2}\frac{d}{dt}\left(u_e \delta_1^*\right) - \frac{\partial \theta_1}{u_e}\frac{\partial u_e}{\partial s}\left(2+H\right) + \frac{C_f}{2} + s_w p_r \frac{2R_O l}{u_e c}\delta_2^* \tag{10}$$

$$\frac{\partial \theta_2}{\partial s} = -\frac{2\theta_2}{u_e}\frac{\partial u_e}{\partial s} + tan\beta_w \frac{C_f}{2} - \frac{1}{u_e}\frac{\partial u_e}{\partial r}\left(2\delta_3 + \delta\right) + \frac{l}{c}\left(\theta_1 + \delta_1^* - \delta - \delta_3 + s_w p_r \frac{2R_O}{u_e}\left(\delta - \delta_1^*\right)\right) \tag{11}$$

In the laminar flow region, the solution of the integral form of the $r-$ momentum Equation 10 is obtained using Twaites' method while in turbulent flow region, the solution of the integral form of the $r-$ and $\theta-$momentum Equations 10 and 11 is carried out using a set of three dimensional turbulent closure relations for the streamwise and spanwise boundary layer variables.

The coupling between the viscous and inviscid parts in $MIRAS$ is done locally for each of the spanwise stations through the transpiration function using the angle of attack calculated upstream the blades leading edge to set the viscous computations. Q^3UIC is used to compute the boundary layer parameters and obtain the chordwise distribution of the transpiration velocity at the center line of the discrete spanwise sections. Q^3UIC computations are performed for the given sectional airfoil geometry at the calculated angle of attack using the following non-dimensional parameters: Reynolds number, $Re = \sqrt{(\Omega r)^2 + (Q_w)^2}\, c/\nu$, ratio between rotational speed and relative velocity, $R_O = \Omega r / U_{rel}$ and ratio between chord length and radial position, $l = c/r$.

The transpiration velocity is computed using the following expression,

$$w_T = \frac{1}{\rho}\frac{\partial}{\partial s}\left(\rho u_e \delta_1^*\right) \tag{12}$$

w_T is introduced in the three dimensional panel method as a source distribution, which acts blowing outwards the limiting streamlines, mimicking the effect of a viscous boundary layer around the blade contour.

3 Results

In this section results obtained with the $MIRAS$ code for the DELFT model rotor, the MEXICO rotor and the virtual NREL 5MW rotor will be presented.

DELFT model rotor

In this section $MIRAS$ simulations of flows past the DELFT model rotor, Figure 1, are compared against hot-film measurements performed by Sant [17] in the open jet wind tunnel of Delft University of Technology. The two bladed DELFT rotor has a radius of $0.6\ m$. The blade has a constant chord of $0.08\ m$ and varying twist angle, constructed using NACA 0012 airfoil along the full blade span. The incoming wind speed in the presented simulations is $5.5\ ms^{-1}$ while

the blades are rotating at a constant angular velocity of $73.3\ s^{-1}$. A surface mesh consisting of 20 spanwise cells and 50 chordwise cells has been used for the $MIRAS$ simulations.

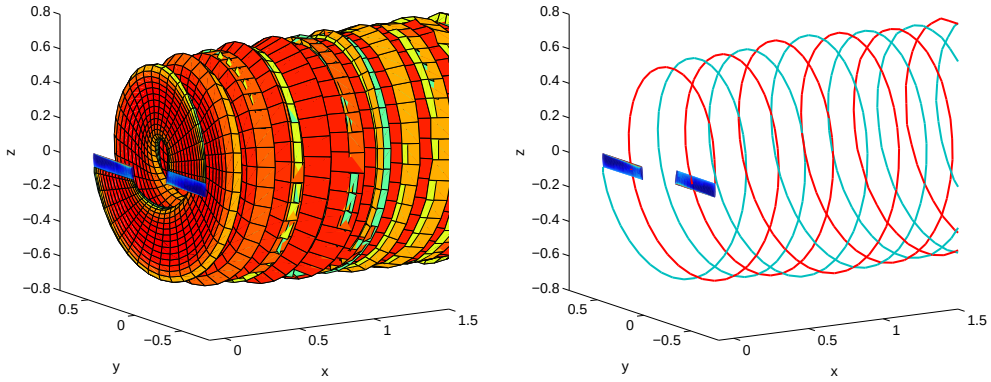

(a) (b)

Figure 1: The wake behind the DELFT rotor at $TSR = 7.96$ (a) full free wake (b) tip vortex filaments.

In Figure 2, the viscous and inviscid axial velocity predictions computed with $MIRAS$ are compared against measurements at distances of $3.5\ cm$ and $9\ cm$ downstream of the rotor plane at a radial location of $0.6R$ along the azimuthal direction from 0 to 360 degrees. Small differences arise between the viscous and inviscid simulations, and the viscous solution is closer to experimental data at the $3.5\ cm$ locations and vice versa at $9\ cm$. Simulations capture pretty well the axial velocity step created by the passage of the blade at the azimuthal positions of 180 and 360 degrees.

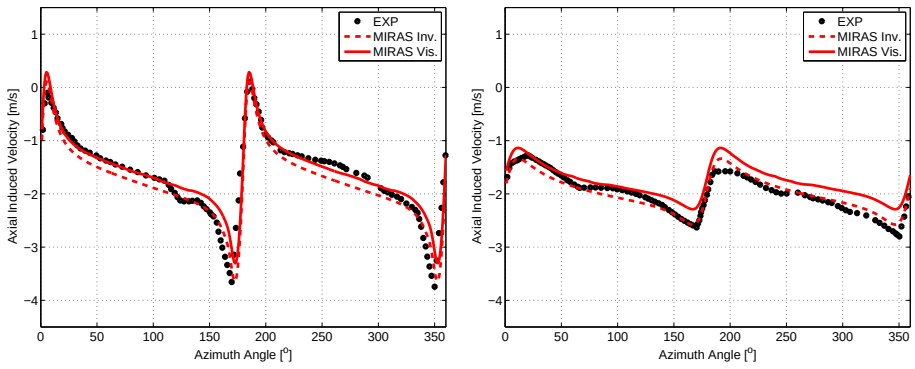

(a) (b)

Figure 2: Axial induced velocity along the azimuthal direction at (a) $3.5\ cm$ and (b) $9\ cm$ downstream of the rotor and a radial location of $0.6R$.

In Figure 3, $MIRAS$ predictions are compared against the measurements performed at a

radial location of $0.9R$ and two downstream positions. Calculated induced velocities are in good agreement with measurements at the $3.5\ cm$ location, implying therefore that the correct rotor loading was predicted. Larger differences can be appreciated at $9cm$, where inviscid simulations are closer to experiments. The more concentrated tip vortices computed in simulations and perhaps a deficient prediction of the wake filaments development near the tip region could give rise to such increasing mismatches between viscous, inviscid simulations and experiments with the downstream location. The use of a finer angular and spanwise discretization or even an adaptative mesh approach could improve the vortex roll-up characteristics.

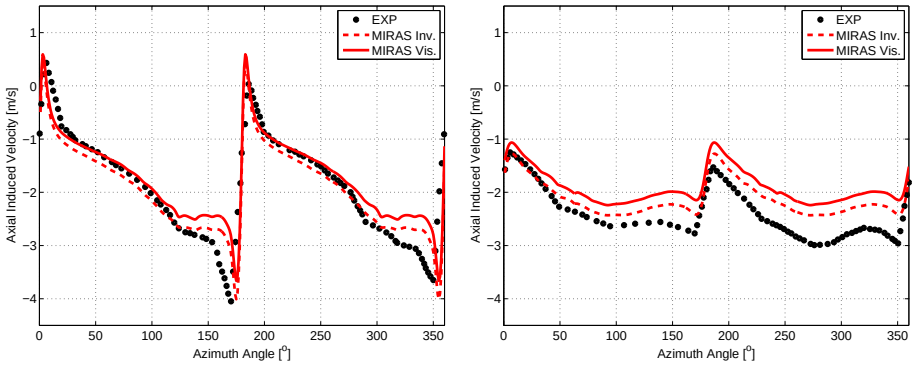

(a) (b)

Figure 3: Axial induced velocity along the azimuthal direction at (a) $3.5\ cm$ and (b) $9\ cm$ downstream of the rotor and a radial location of $0.9R$.

The calculated wake vortex filaments for the viscous simulations presented above are shown in Figure 4. The influence of the wake passage crossing through the hot-film sampling vicinity is clearly seen at the $0.9R$ locations around 180 and 360 degrees, although its influence diminish with the decreasing radial location due to the weaker vortices shed in that region.

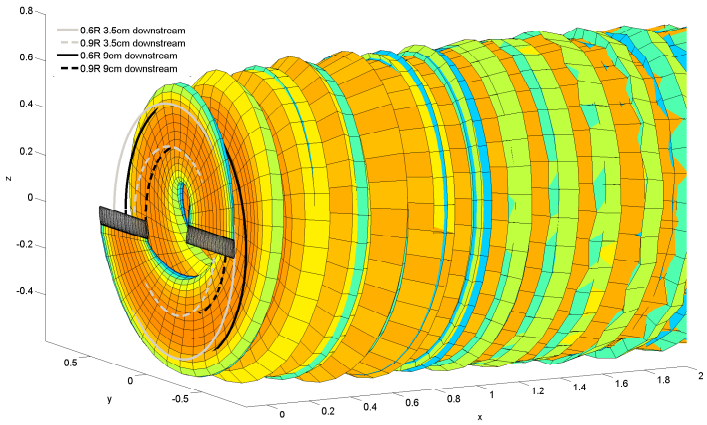

Figure 4: Calculated wake filaments for the DELFT rotor including hot-film location.

MEXICO model rotor

A further validation of the viscous and inviscid versions of the $MIRAS$ code is carried out for flows past the MEXICO rotor, Figure 5. In what follows the blade normal and tangential forces are compared against measurements and wake velocities are validated against PIV experimental data.

The MEXICO experiment was executed on a three-bladed wind turbine model with a diameter of $4.5\,m$ under controlled conditions in the Large Scale Low Speed Facility of the German-Dutch Wind tunnel Organization DNW with a $9.5\ X\ 9.5\ m^2$ open test section. The test cases considered here are the rotor rotating with a constant angular speed of $424.5\,rpm$ at wind speeds of 10, 15 and $24\ ms^{-1}$. The blades are subjected in all the three cases to a negative collective pitch of $\delta_0 = -2.3°$. Instantaneous velocities were extracted in a plane at 9 o'clock when looking downstream at the rotor when the first blade pointed upwards. For more detailed information about the MEXICO experiment campaign the reader is referred to Schepers and Snel [18].

A surface mesh consisting of 20 spanwise cells and 50 chordwise cells was used for $MIRAS$ simulations. Laminar to turbulent transition was forced at a 5% of the chord from the leading edge on both the upper and lower sides of the airfoil sections.

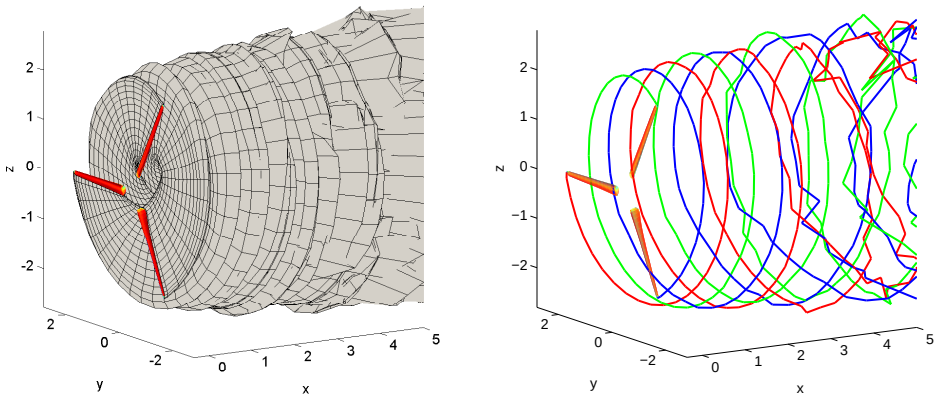

(a) (b)

Figure 5: MEXICO rotor at $TSR = 6.67$ (a) full free wake (b) Tip vortex filaments.

In Figure 6, the predictions of the normal an tangential blade forces are compared against experimental values for the wind speeds cases of 10, 15 and $24\ ms^{-1}$. As the wind speed increases the inviscid computations predict higher values of both normal and tangential forces while the viscous simulations are in much better agreement with experiments, except in the root region where rotational effects arising from Coriolis and centrifugal forces seem to be underpredicted. At $24\ ms^{-1}$ differences between the viscous and inviscid predictions are enormous, this is related to the existence of regions with trailing edge separation.

In Figures 7 and 8 $MIRAS$ viscous and inviscid predicted velocities are compared against PIV measurements in axial and radial traverses for a wind speed of $24ms^{-1}$. Viscous simulations

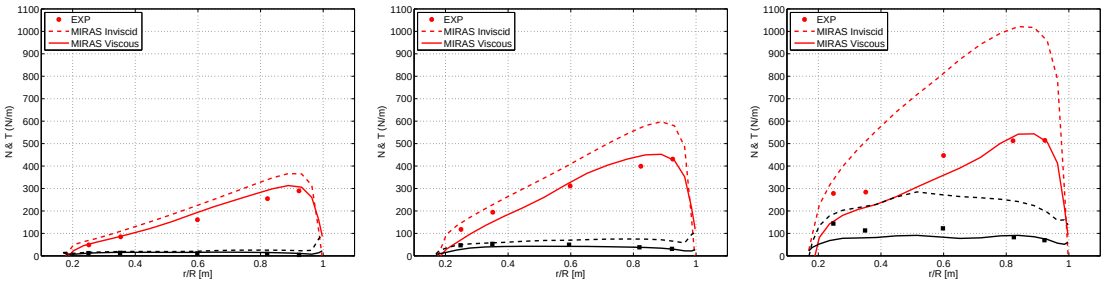

(a) (b) (c)

Figure 6: Blade normal and tangential forces at wind speeds of (a) 10, (b) 15 and (c) 24 ms^{-1}.

capture much better the axial velocities while the radial and tangential ones are more difficult to predict. Overall a good agreement was obtained against experiments in all the cases.

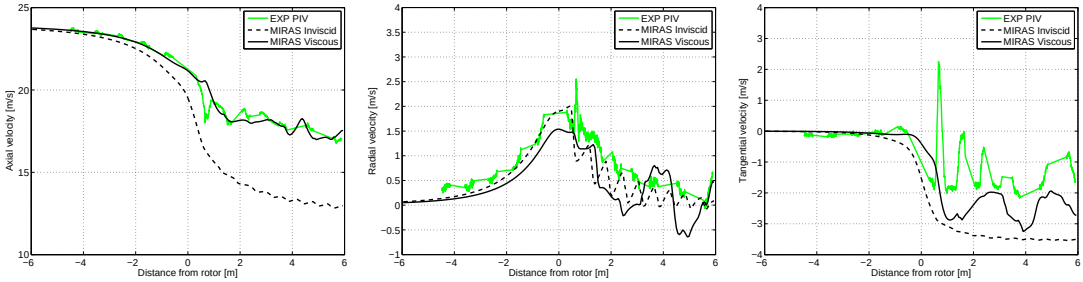

(a) (b) (c)

Figure 7: (a) Axial, (b) radial and (c) tangential velocities in an axial traverse of z = 1.38 m at a wind speed of 24 ms^{-1}.

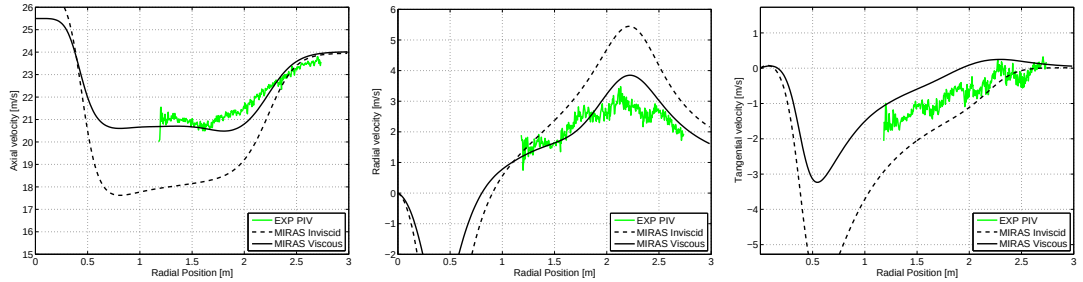

(a) (b) (c)

Figure 8: (a) Axial, (b) radial and (c) tangential velocities in a radial traverse of x = 0.30 m at a wind speed of 24 ms^{-1}.

NREL 5 MW virtual rotor

In this section $MIRAS$ simulations are compared against Navier-Stokes computations for the NREL 5 MW virtual wind turbine. The CFD computations were carried out using the $EllipSys3D$ code in fully turbulent mode with the $k-\omega$ SST turbulence model [19]. The mesh used by EllipSys3D is a cylindrical mesh of $4.2 \cdot 10^6$ mesh points which covers a domain with a radius of $245\ m$ and inlet and outlet located at $287\ m$ in front and behind the rotor. A surface mesh consisting of 20 spanwise cells and 50 chordwise cells has been used in this case and 14 wake revolutions were simulated with an angular discretization of $10°$.

The wake calculated in $MIRAS$ simulations, Figure 9, shows an important wake expansion and it can be appreciated how the interaction between the vortex sheets breaks the smooth shape of the wake as it moves downstream. This effect is clearly observed when following the vortex filaments released from the blades tip, Figure $9(b)$. After two wake revolutions the blade to blade filament interaction grows and generates a vortex pairing phenomena which makes the filaments tangle with each other as they move further downstream.

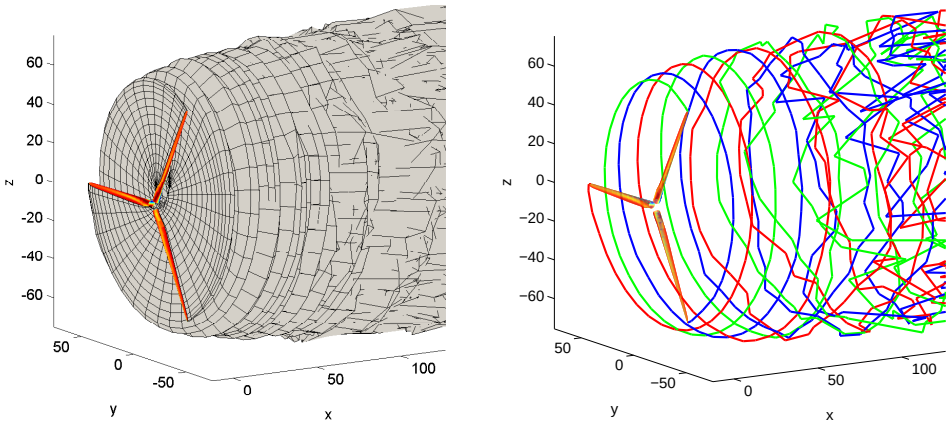

(a) (b)

Figure 9: (a) Full free wake (b) Tip vortex filaments of flows pass the NREL 5MW rotor at a $TSR = 6.65$.

Predicted normal and tangential forces are compared for the cases at wind speeds of $6\ ms^{-1}$ and $10\ ms^{-1}$, Figures 10 and 11. In terms of normal forces $MIRAS$ viscous predictions are in excellent agreement with CFD data, while the inviscid ones are overpredicted as expected. From the figures, it is seen that viscous simulations underpredict the tangential force near the blade tip region at the higher wind speed case, $10\ ms^{-1}$, although a better agreement is obtained at $6\ ms^{-1}$.

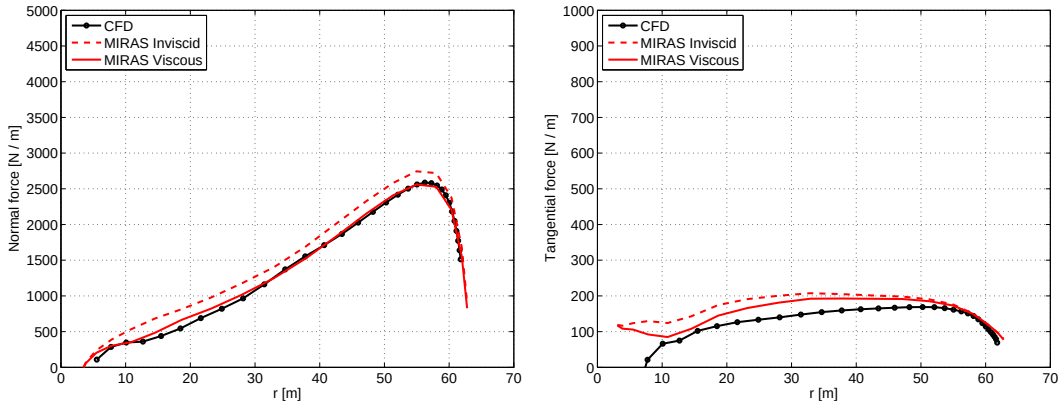

(a) (b)

Figure 10: (a) Normal and (b) tangential forces on the NREL 5MW blades. Viscous and inviscid $MIRAS$ and Navier-Stokes $EllipSys3D$ simulations for $6\,ms^{-1}$.

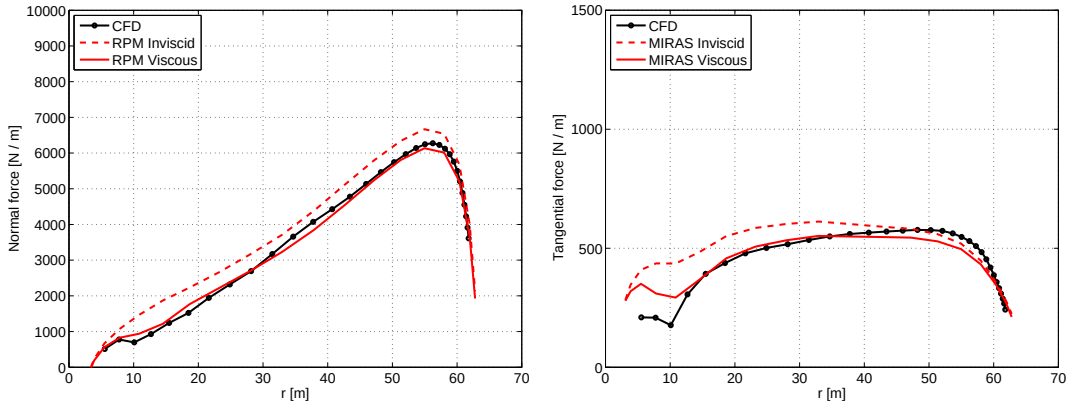

(a) (b)

Figure 11: (a) Normal and (b) tangential forces on the NREL 5MW blades. Viscous and inviscid $MIRAS$ and Navier-Stokes $EllipSys3D$ simulations for $10\,ms^{-1}$.

4 Conclusion

The $MIRAS$ code, an unsteady three-dimensional panel method coupled with the integral boundary layer solver Q^3UIC has been presented and validated against experiments and CFD simulations for three different wind turbine rotors.

Near wake axial velocities computed with $MIRAS$ have been compared with hot-film measurements for the DELFT model wind turbine obtaining a good agreement.

Computed axial, radial and tangential velocities have been validated against MEXICO PIV measurements, as well as normal and tangential blade forces.

To conclude the study, $MIRAS$ simulations of the virtual NREL 5 MW wind turbine have been compared against Navier-Stokes simulations in terms of blade forces, obtaining an excel-

lent agreement for the normal forces and a fairly good comparison for the tangential ones.

5 Acknowledgements

We gratefully acknowledge the support from the Danish Council for Strategic Research for the project 'Center for Computational Wind Turbine Aerodynamics and Atmospheric Turbulence' (2104-09-067216/DSF), the Energy Technology Development and Demonstration Program (EUDP-2011-64011-0094) and the Danish Energy Agency (EUDP-2012-64012-0146).

References

[1] J.L. Hess 1971 Numerical solution of inviscid subsonic flows *Von Karman Institute for Fluid Dynamics, Lecture Series,* ***34***

[2] J. Katz 1985 Calculation of the Aerodynamic Forces on Automotive Lifting Surfaces *Transactions of the ASME,* ***107****: 438–443*

[3] L. Morino, Z. Kaprielian and S.R. Sipcic 1985 Free Wake Analysis of Helicopter Rotors *Vertica,* ***9****: 127–140*

[4] M.J. Lighthill 1958 On displacement thickness *Journal of Fluid Mechanics, vol. 4, pp. 383-392*

[5] N. Ramos-García 2011 Unsteady viscous-inviscid interaction technique for wind turbine airfoils *PhD. Thesis, Technical University of Denmark, Department of Mechanical Engineering, ISBN 978-87-90416-53-9*

[6] N. Ramos-García, W.Z. Shen and J.N. Sørensen 2013 A Strong Viscous-Inviscid Interaction Model for Rotating Airfoils *Submitted to Wind energy*

[7] J. Katz and A. Plotkin 1977 Low speed aerodynamics *McGraw-Hill, second edition*

[8] J.G. Leishman 2000 Principles of Helicopter Aerodynamics *Cambridge University Press*

[9] S. Ananthan and J.G. Leishman 2004 Role of Filament Strain in the Free-Vortex Modeling of Rotor Wakes *Journal of the American Helicopter Society*

[10] T. Cebeci, M. F. Platzer, H. M. Jang and H. H. Chen 1993 An inviscid-viscous interaction approach to the calculation of dynamic stall initiation on airfoils *Journal of Turbomachinery,* ***115****: 714-723*

[11] J. N. Sørensen 1988 Prediction of Separated FLow Past Airfoil using Viscous-Inviscid Interaction Technique *La Recherche Aerosptatiale 1-11*

[12] M. Drela and M. B. Giles 1987 Viscous-inviscid analysis of transonic and low Reynolds number airfoil *AIAA journal **25**: 1347–1355*

[13] J.G. Leishman, M.J. Bhagwat and A. Bagai 2002 Free-Vortex Filament Methods for the Analysis of Helicopter Rotor Wakes *Journal of Aircraft **5**: 759–775*

[14] M.P. Scully 1975 Computation of Helicopter Rotor Wake Geometry and Its Influence on Rotor Harmonic Airloads *Ph.D. Thesis, Massachusetts Institute of Technology. Dept. of Aeronautics and Astronautics*

[15] H.B. Squire 1965 The growth of a vortex in turbulent flow *Aeronautical Quarterly **16**: 302–306*

[16] M.J. Bhagwat and J.G. Leishman 2001 Accuracy of Straight-Line Segmentation Applied to Curvilinear Vortex Filaments *Journal of the American Helicopter Society **46**:2:166-169*

[17] T. Sant 2007 Improving BEM-base Aerodynamic Models in Wind Turbine Design Codes *PhD Thesis, ISBN: 978-99932-0-483-1, Delft University Wind Energy Research Institute*

[18] J.G. Scheepers and H. Snel 2007 Model Experiments in Controlled Conditions Final Report *The Energy Research Center of the Netherlands The Energy Research Center of the Netherlands*

[19] W.Z. Shen, W.J. Zhu, J.N. Sørensen, N.N. Sørensen and P.E. Réthoré 2012 Study of tip loss corrections using CFD rotor computations *The Science of Making Torque from Wind, Oldenburg*

[20] T. Cebeci, D. Sedlock, K.C. Chang and R.W.Clark 1988 Analysis of Wings with Flow Separation *Journal of Aircraft, **26**:3:214-220*

[21] U.J. Pesonen, R.K. Agarwal and S. Laine 2000 Fast and Robust Viscous/Inviscid Interaction Code for Wing Flowfield Calculations *Journal of Aircraft, **37**:4:730-733*

[22] L.A. Lemmerman and V.R. Sonnad 1979 Three-Dimensional Viscous-Inviscid Coupling Using Surface Transpiration *Journal of Aircrfact, **16**:6:353-358*